

An Investigation of Viscoelastic Fluid-Structure Interaction

Chirag Chauhan¹, Somvir Arya²

¹Research Scholar, Mechanical Engineering Department, Indus Institute of Engineering & Technology, Kinana (Jind) Haryana India

²Assistant Professor & Head, Mechanical Engineering Department, Indus Institute of Engineering & Technology, Kinana (Jind) Haryana India

Abstract: It is well known that when a flexible or flexibly-mounted structure is placed perpendicular to the flow of a Newtonian fluid, it can oscillate due to the shedding of separated vortices at high Reynolds numbers, if the same flexible objects are placed in non-Newtonian flows; however the structure's response is still unknown. The main objective of the work is introduce a new field of viscoelastic fluid-structure interactions by showing that the elastic instabilities that occur in the flow of viscoelastic fluids can drive the motion of a flexible structure placed in its path. In this work are the results of an investigation of the interaction occurring in the flow of a viscoelastic wormlike micelle solution past a flexible rectangular sheet. The structural geometries studies include: flexible sheet inclination at 20°, 45°, 90° and flexible sheet width of 5mm and 2.5mm. By varying the flow velocity the response of the flexible sheet has been characterized in terms of amplitude and frequency of oscillations. Steady and dynamic shear rheology and filament stretching extensional rheology measurement are conducted in order to characterize the viscoelastic worm like micelle solution.

1. Introduction:

When a flexible or flexibly mounted structure is placed in the path of fluid flow, the fluid exerts a force on the structure which causes the structure to deform. This deformation of the structure in turn modifies the fluid forces exerted by the fluid flow. This leads to a coupling between structural motion and the fluctuating fluid forces. This constitutes a fluid-structure interaction (FSI). The field of FSI has many applications in harnessing wind energy, novel energy extraction methods and biomedical engineering. The fundamental studies on FSI for Newtonian fluid have been collected in the form of several books and review papers. Of all these studies, here we will focus on a model FSI problem Vortex-Induced Vibration (VIV).

Keywords: Viscoelastic, fluid, Structure, Interaction, Newtonian

2. Literature:

The case of a long flexible cylinder in a cross-flow has been considered only re-cently due to its complexities. These complexities are associated with the distributed interaction between the fluid and the flexible body, including the difficulty to pin-point the region where the fluid excites the body, and identifying the mechanisms of energy redistribution along the span. Detailed laboratory experiments on flexible structures placed in flow have provided information on the amplitude of vibration, excited frequencies and structural wave numbers [6]. For long flexible cylinders, contrary to the case of rigid cylinders, the phase difference between the in line and cross flow displacement scan vary along the span, leading to diverse trajectories along the structure [7-9]. A dominant mechanism has been identified in the interaction between a flexible circular cylinder undergoing free vibrations in sheared cross flow and the vortices forming in its wake energy is transferred from the fluid to the body under a resonance condition, which occurs within a well-defined region of the span, dominated by counter clockwise, figure-eight orbits [4]. In all the cases of FSI described above, the fluid was Newtonian and the flow was at moderate to high Reynolds numbers, $Re > 50$. In these inertial-dominated flows, the motion of the cylinder was driven by the shedding of vortices which separate from the cylinder and shed from its wake. There are however, a whole class of flows in which the Reynolds number is vanishingly small, inertia plays essentially no role and yet the flows can become unstable. In these cases, the presence of high molecular weight polymers or wormlike micelle scan makes the fluids elastic. The combination of fluid elasticity and mean curvature of the stream lines has been shown to destabilize the flow and lead to the onset of elastically-driven How instabilities [10]. In this study, we present results that show that these instabilities can drive the motion of a flexible structure placed in its flow path.

3. Objective of the study:

The goal of this work is to study fluid-structure interaction (FSI) phenomena in which the fluid is a non-Newtonian viscoelastic fluid and the structure is flexible. FSI has been studied extensively for structures in contact with Newtonian fluid where the shedding of separated vortices at high Reynolds numbers can drive the motion of a flexibly-mounted or flexible structure. An example is the use of carbon fiber reinforced polymer composites. With the push to higher fuel economy standards, reducing the weight of cars and airplanes while maintaining their structural integrity is highly desirable. Carbon fiber reinforced composite parts are formed by driving a polymer resin through a woven carbon fiber

mat. At the high flow rates desired to make this process economically competitive, the viscoelastic polymer in fluid can experience elastic flow instability. This flow instability can drive the motion of the carbon fiber matrix even failure of the fibers. Here the FSI Between a flowing viscoelastic fluid and one or more elastic solid fibers is critically important to the success of an injection mold ed part.

4. Experimental Setup:

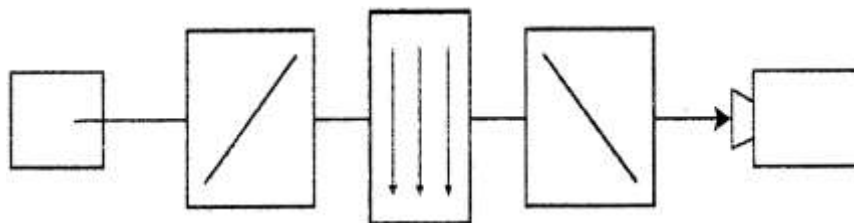
4.1 Flow-induced birefringence (FIB):

The refractive index of a wormlike micelle varies depending on whether the light passes parallel or normal to the micelles backbone. By passing light of a known polarization state and frequency through a fluid sample and measuring the resulting change in polarization state, flow-induced birefringence takes advantage of this fact to measure the deformation of the micelle. Under all flow conditions, this technique can at least qualitatively elucidate the regions of large stress in a flow. In the limit of small deformations, an optical train can be built up using Mueller calculus, and a value of the micelle deformation can be calculated from as tress- optic coefficient. Flow- induced birefringence measurements have been used quite extensively to examine both steady and transient How so flows and wormlike micelles [16- 19]. A mono chromatic light source was used to illuminate the How between crossed polarizers. A Nikon D70 digital camera was used to capture the birefringent patterns in the wormlike micelle solution generated by the flow for each linear polarizer configuration. Due to the extreme deformation the micellar network undergoes at high Deborah numbers, data analysis becomes impractical because the birefringence quickly gum through orders. The full field FIB technique is used only qualitatively to highlight the deformation. It is a visualization tool to aid the observer.

5. Result & Discussion:

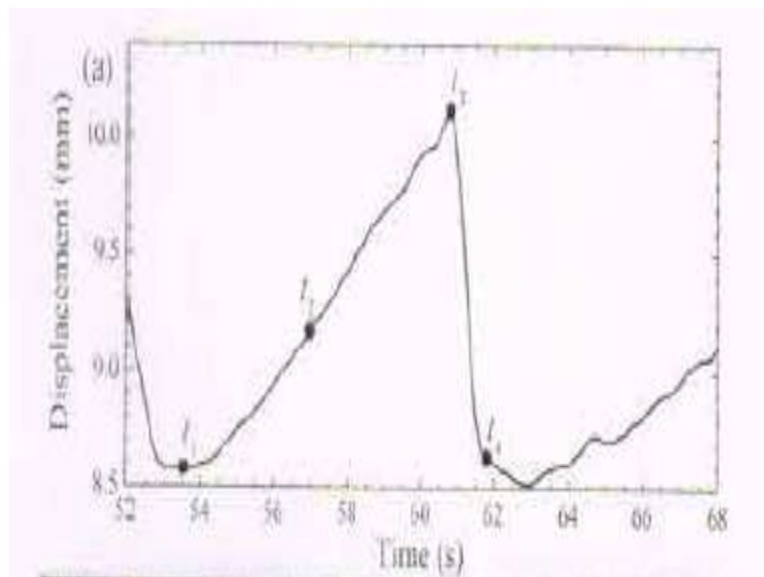
5.1 Flow-induced birefringence (FIB):

Full-field flow-induced birefringence measurements were made using the crossed polarizer technique described in [28]. The areas of large micellar deformation are clearly seen in Fig.3.6 at a flow velocity of $U = 4.3\text{mm/s}$. The polarizers have been oriented at 45° and 135° and the regions of extensional deformation are high-lighted.



Light source Polarizer at 45 'Flow cell Polarizer at35° Camera

Figure 1. Schematic diagram of the setup used to obtain flow induced birefringence images in this study



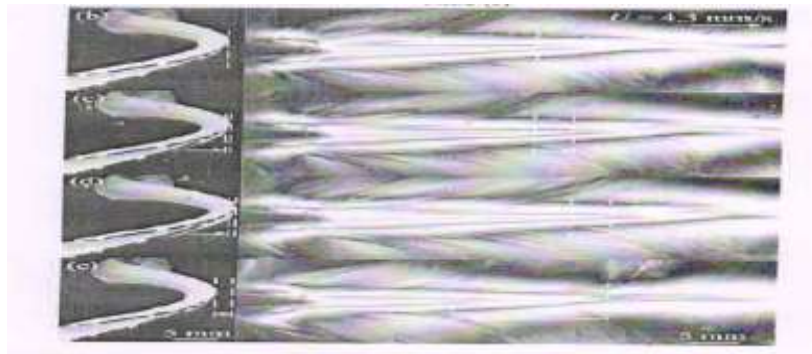


Figure 2 (a) Time history of the center line deflection of the sheet for one period of oscillation. Together with bright field images of deformed sheet (left), and the extensional birefringent patterns obtained by setting the crossed polarizers at 45° and 135° (right) at $U=4.3\text{mm/s}$ and for (b) $t_1=0$, (c) $t_2=3.45\text{s}$, (d) $t_3=7.2\text{s}$, and (e) $t_4=7.95\text{s}$. The dashed lines highlight the difference in the extensional birefringence patterns and deformations of the sheet between each time interval.

It is known that in flows with stagnation points, that a narrow region of high polymer or micelle deformation known as birefringent strands can form in the strong extensional flow just downstream of the stagnation point [29,30]. These birefringent strands appear as bright areas or fringes directly in the wake of the flexible sheet. These fringe patterns are in excellent agreement with the patterns observed in both experiments [31] and numerical simulations [32, 33]. In Fig. 2 the birefringence quickly goes through orders, here seen as rainbow fringe patterns, indicating a substantial amount of deformation and thus stress accumulated by the fluid as it flows past the flexible sheet. Because of this, it is impossible as a practical matter to obtain a quantitative value of the extinction and retardation angles from which to calculate a value of stress. Additionally, under such large deformations, the linear stress-optic rule no longer holds, and thus the birefringence data is used only as a qualitative tool to guide the eye. However it is still qualitatively an excellent tool to examine the stress and deformation fields generated by the flow around the flexible sheet during its time dependent fluctuations. As seen in Fig. 2, a narrow region of micelle deformation, known as a birefringent tail, forms in the strong extensional flow region just downstream of the stagnation point. In the wake, the fluid must accelerate from rest along the trailing edge of the sheet to the maximum flow velocity U_{max} : over a short distance downstream of the flexible sheet. This extensional flow results in strong micelle alignment and deformation as seen in Fig. 2 (b). As the flow velocity is increased, a stable birefringence tail grows both in length and intensity until the onset of the viscoelastic flow instability. After the set of the flow instability, the maximum extent of the birefringent tail approaches an asymptotic limit. A series of dashed lines have been added to Fig. 2 to graphically illustrate the magnitude and direction of the changes to the birefringence pattern with time during one oscillation cycle. A similar line has been added to show the deflection of the sheet in the bright field images to the left of the FIB. At the start of an oscillation (Fig. 2 (b)), the wormlike micelle solution already exhibits a significant amount of extensional stress in its wake. The birefringent tail grows in length and intensity with time (Fig. 2 (c)) resulting in still further stretching of the flexible sheet. At its maximum extent (Fig. 2 (d)), the birefringence has grown by approximately 30% beyond its minimum extent (Fig. 2 (b)) to nearly 10H downstream, while the deflection of the sheet has increased by roughly 12% from 8mm to 10mm. When the displacement of the sheet reaches 10mm, a abrupt breakdown of the wormlike micelles in the high stress wake is observed resulting in a rapid loss of extensional stress in the wake. This can be seen in Fig. 2 (e) as a significant reduction in the length and extent of the birefringent tail. The start of the next oscillation cycle corresponds not to the flow of new unaffected wormlike micelles from upstream of the flexible sheet into its wake where they begin to stretch and deform the flexible sheet again. Similar FIB patterns were observed at all flow velocities where the flow of wormlike micelle solution was found to become unstable.

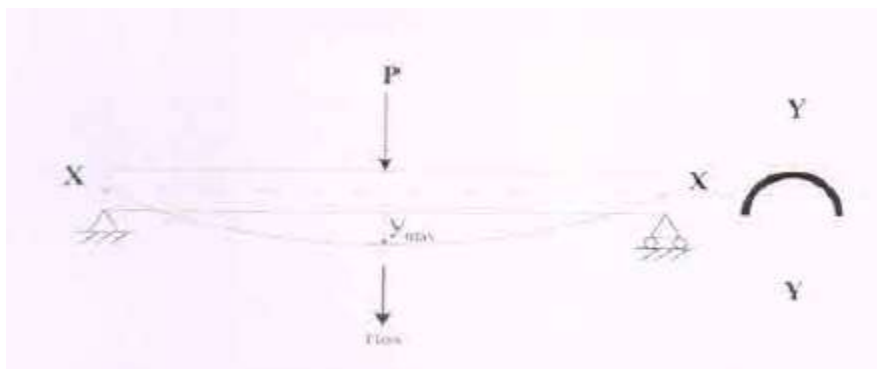


Figure 3 The span wise deformation of the flexible sheet during the oscillation cycle

5.2 Flexible sheet deformation and extensional fluid stresses:

It can observe that the flexible sheet does not only undergo as pan wise deformation but also a complex 'C' shaped curvature seen in the cross section. Thus, in order to correlate the extensional stress developed in the fluid in the wake to the total stress applied on the flexible sheet ,it is important to take into consideration the total deformation of the flexible sheet in line and also cross How to the flow direction. To simplify calculations, we have estimated the stress experienced by the flexible sheet in separate cases, that is, in the in line and cross flow directions, even though the resulting deformation occurs simultaneously and thus is quite a complex occurrence. The stress required for the in-line sheet deformation can be calculated by assuming the sheet to be a simply supported beam with a 'C' cross section profile and using Euler's beam theory to estimate the maximum force applied in the mid section at the maximum observed displacement of the sheet. Thus, the force at the midsection of the flexible sheet for only in line deformation is given by.

$$P = Yma \frac{48EI}{L^3} \tag{1}$$

Where P is the load acting on the midsection, $Yma_{11} = 11\text{mm}$ is the maximum midsection flexible sheet displacement, $E = 0.1 \times 10^6 \text{ Pa}$ is the elastic modulus of the flexible Sheet and $I = 0.48\text{mm}^4$ is the second area moment of inertia of the 'C' shaped cross section of the flexible sheet.

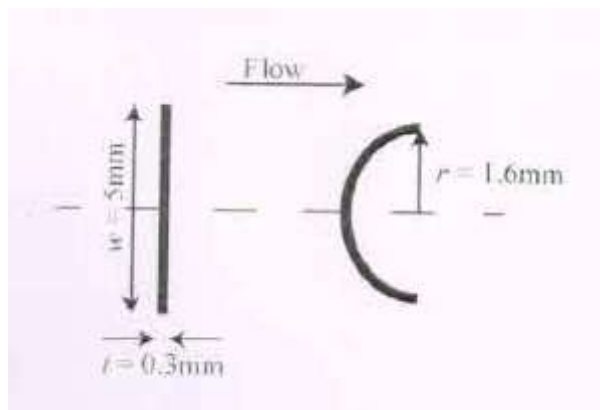


Figure 4 The assumed semicircular cross section profile of the flexible sheet during the oscillation cycle

Times, the stress experienced due to an in line force acting on the flexible sheet can be found,

$$\tau_{inline} = \frac{P}{L \times B} = 5Pa \tag{2}$$

Where $L \times B$ is the area of the flexible sheet exposed to the incoming time. In addition to bending, there is a tensile stress which results from the sheet stretching from its initial undeformed state to its deformed elongated contour length at maximum deflection. By calculating the strain, E , from the images of the deformed sheets, this stress was found to be approximately

$$\sigma_{tensile} = E\epsilon = 13kPa$$

The stress required to bend the flexible sheet cross section into a 'C' profile results in tensile elastic force acting on the outer layer of the sheet. This tensile stress on the flexible sheet is estimated below.

Distance from neutral axis, $c = 0.15\text{mm}$

$$\epsilon_{neutral} = \frac{c}{r} = \frac{0.15\text{mm}}{1.6\text{mm}}$$

$$\tau_{crossflow} = E\epsilon_{neutral} = 9\text{kPa}$$

From filament stretching extensional rheology measurements, the wormlike micelle solution was found to rupture and fail at an extensional stress of 7kPa. Thus, these calculations appear to confirm that the viscoelastic fluidic stresses needed to deform the sheet are large enough to resulting break down of viscoelastic wormlike micelles in the wake of the sheet resulting in a time-dependent flow field, which in turn drives the observed time-dependent oscillations of the sheet. It is important to note that this is a simplified explanation of the oscillation mechanism. As the cross flow and in line deformation occur together, it can lead to changes in the sheet properties like the area moment of inertia and the cross section of the flexible sheet does not stay a shape across the sheet span throughout a period of oscillation.

Conclusion:

For a stable velocity, the extensional stresses produced by the wormlike micelle solution in the wake of the flexible sheet produced a static deflection of the flexible sheet. Beyond a critical flow velocity while at an infinitesimal Re , the fluid was found to show elastic instabilities, resulting in periodic fluctuating stresses in the wake of the flexible sheet. These periodic elastic instabilities have been observed in a number of studies using this test fluid [28, 34]. However, in this study these elastic instabilities occur in the wake of a flexible sheet which imparts a periodic fluctuating stress on the structure too. The flexible sheet was found to have periodic oscillations with a saw tooth-like pattern seen in a time history plot. A bifurcation diagram is presented to show the progressing of the amplitude of the flexible sheet oscillation about its mean center line deflection. From the amplitude and frequency plots, it is found that amplitude of oscillation grows linearly until a maximum. This trend has been attributed to the varying difference between the growth rate of stresses in the fluid which is dependent on the two velocities and the recoil, Rate of the flexible sheet which is a structural property. A long with this transition comes the change in the dominance of local fluid elastic instabilities instead of a global central instability with increasing tow velocity flow induced birefringence images show the transition of slow growth and rapid decay of extensional stresses in the wake of the flexible sheet in terms of the changing length and intensity of the birefringent tail observed in the wake. Additionally, there is no vortex shedding observed during the oscillation cycles as is common in Newtonian FSI studies. The complex deformation that the flexible sheet undergoes during each cycle of oscillation has been highlighted in the bright field images. These images indicate the in line and cross-flow deformation that occur simultaneously with increasing extensional stresses produced by fluid flowing past the sheet. An analysis of the stresses required to produce the sheet deformation has been conduct. In order to correlate the extensional stress in the fluid with the stress required to produce the observed deformation of the flexible shed. 11. Has been shown that the tensile stress and needed for the in-line stretching of the flexible sheet all the stress are found to be of the flexible sheet into a complex $\cdot c \cdot$ shape is many times greater than that required for the in-line bending of the sheet span. These stresses are found to be close to the magnitude of the maximum elastic normal stresses that can be supported by the fluid before the stretched and deformed micelles in the solution fail. We are able to conclude that there is a strong relation between the observed magnitude of flexible shed deformation and the maximum elastic tensile stresses reached before filament failure studies through filament stretching extensional rheology measurements performed on this solution.

In conclusion, we have shown, for the very first time. That pure elastic flow instabilities occurring in a viscoelastic fluid flow can drive the motion of a flexible structure placed in its path. The oscillations of the flexible structure, which develop at infinitesimal Reynolds numbers and in the absence of vortex shedding, have been presented for three inclinations and two width variations of a flexible sheet.

REFERENCES:

- [1] T. Prasauth and S. Mittal. Vortex- induced l vibrations of a circular cylinder at low Reyn olds numbers." *Joiu. nal of F foild Mechanics*, vol.594,p.463,2008.[28] D. Jeon and M. Gharib. "On circular cylinders under going two-degree-of-freedom forced motions. " *Journal of fluids and Structures*, Vol. 15 no. 3 pp 533-541 2001
- [2] N. Jauvtis and C. Williamson, "The effect of two degrees of freedom on vortex- induced vibration at low mass and damping, " *Journal of Fluid Mechanics*, vol.509,no.6, pp. 23--62,2004.
- [3] J.M. Dahl, F.S.Hover, M.S.Triantafyllou. S.Dong, and G.E. Karniadakis, "Resonant vibrntions of bluff bodi es cause multi vortex shedding and high fre- quency forces." *Phys. Reu. Lett.* vol. 99,p. 144503, Oct 2007.
- [4] J. DahL F. Hover, M. Triantafyllou, and O. Oakley, "Dual resonance in vortex- induced vibrations at subcritical and super critical reynolds numbers," *Journal of Fluid Mechanics*. vol. G43,n0. 1,pp. 395--424,2010.
- [5] A. Trim, H. Braaten. H. Lie. And IV I. Tognarelli, "Experimental investigation of vortex induced vibration of long marine risers. " *Journal of fluids and structures*, vol. 21. no. 3. pp. 335—3 (i1.2005.
- [6] J. K. Vandiver, V. faiswaL and V. Jhingran, "Insight son vortex induced, traveling wave son long risers, " *Journal of Fluids and Structures*, vol.25,no.4, pp. 641-653,2009.
- [7] Y. Modarres-Sadeghi, H. Ivlukundan. J. Dahl, F. Hover. and M. Triantafyllou, "The effect of higher harmonic forces on fatigue life of marine risers, " *Journal of Sound and Vibration*, vol. 329, no. 1,pp. 43-55,2010.
- [8] R. Bourguet, G.E. Karniaclakis, and. M.S. Triantafyllou, "Distributed lock in Jrivesbrud band vortex induced vibrations of along flexible cylinder in slwar flow, " *Jomal of Fluid Mechanics*. vol. 717. pp. 361-375,2013.
- [9] G.H. McKinley. P. Pakele and A. Oztekin. "Rheological and geometrics caling of purely elastic flow instabilities *J. Non-Newtonian Fluid Mech.* ,vol.67, pp. 19-47,199G.
- [10] K. fakenchi, Y. Majima. .K. Hiratcl A. Morishita, M. Hattori, and Y. Sakakura. "Viscoelastic properties of middle entr effusions from pediatricotitis media with effusion and their relation to gross appearance, " *Eurvpean Archives of O to Rhino Laryngology*, vol. 247, no. 1,pp. 60--62,1990.
- [11] E. Lauga, "Life at high Deborah number, " *EPL*, vol. 86, p. 64001,2009.
- [12] J. Teran, L. Fanci. And M. Shelley. "Viscoelastic fluid response can increase the speed and efficiency of a free swimmer. " *Phys. Rev. Lett.* vol. 104, p. 03801,2010.

- [13] B. Lin, T. Powers, and K. S. Brener. "Force-free swimming of a model helical flagellum in viscoelastic fluids," *PNAS*, vol. 108, pp. 19516-19520, 2011.
- [14] J. Espinosa-Garcia, E. Langa, and R. Zenit, "Fluid elasticity increases the locomotion of flexible swimmers." *Phys. Fluids*, vol. 25, p. 031701, 2013.
- [15] J. Drappier, D. Bonn, J. Meunier, S. Lerouge, J. Decruppe, and F. Bertrand, "Correlation between birefringent bands and shear bands in surfactant solutions," *J. Stat. Mech. Theory and Exp.*, p. P04003, 2006.
- [16] G. G. Fuller, *Optical Rheometry of Complex Fluids*. New York: Oxford University Press, 1995.
- [17] T. Shikata, S. Dahman, and D. Pearson, "Rheo-optic behavior of wormlike micelles," *Langmuir*, vol. 10, pp. 3470-3476, 1994.
- [18] E. Wheeler, P. Fischer, and G. Fuller. "Time-periodic flow induced structures and instabilities in a viscoelastic surfactant solution," *J. Non-Newtonian Fluid Mech.*, vol. 75, pp. 13-208, 1998.
- [19] R. Bird, R. Armstrong, and O. Hassager, *Dynamics of Polymer in Liquids: Volume Fluid Mechanics*. New York: John Wiley & Sons, 1987.
- [20] P. Fischer and H. Recharge, "Rheological master curves of viscoelastic surfactant solutions by varying the solvent viscosity and temperature," *Langmuir*, vol. 13, pp. 7012-7020, 1997.
- [21] M. Cates, "Reptation of living polymers: Dynamics of entangled polymers in the presence of reversible chain scission reactions," *Macromol.*, vol. 20, pp. 2289-2296, 1987.
- [22] R. Granek and M. Cates, "Stress relaxation in living polymers: Results from a Poisson renewal model." *J. Chem. Phys.*, vol. 96, pp. 4758-4767, 1992.
- [23] M. Doi and S. Edwards. *The Theory of Polymer Dynamics*. Oxford University Press, 1986.
- [24] A. Bhardwaj, D. Richter, M. Chellaiah, and P. Rothstein, "The effect of preshear on the extensional rheology of wormlike micelle solutions," *Rheol. Acta*, vol. 46, no. 6, pp. 861-875, 2001.
- [25] P. Szabo. "Transient filament stretching rheometry: Force balance analysis," *Rheol. Acta*, vol. 36, pp. 277-26-1, 1997.
- [26] J. S. L. Anna, G. H. McKinley, D. A. Nguyen, T. Sridhar, S. J. Muller, J. Huang, and F. James. "An inter-laboratory comparison of measurements from filament stretching rheometers using common test fluids," *J. Rheol.*, vol. 45, no. 1, pp. 83-114, 2001.
- [27] G. R. Moss and J. P. Rothstein. "Flow of wormlike micelle solutions past a confined circular cylinder," *Journal of Non-Newtonian Fluid Mechanics*, vol. 165, no. 2122, pp. 1505-1515, 2010.
- [28] R. Cressely and H. Hocquart. "Localized flow birefringence induced in the wake of obstacles." *Optical. Acta*, vol. 27, no. 5, pp. 699-711, 1980.
- [29] C. Chen and G. Warr, "Light scattering from wormlike micelle solutions in longational flow." *Langmuir*, vol. 13, pp. 1374-1376, 1997.
- [30] F. P. T. Baaijens, S. Selen, H. P. W. Baaijens, G. W. M. Peters, and H. E. H. Meijer. "Viscoelastic flow past a confined cylinder of a low density polyethylene melt." *J. Non-Newtonian Fluid Mech.*, vol. 68, pp. 173-203, 1997.
- [31] M. Chilcutt and J. HAJJISUN, "Creeping flow of dilute polymer solutions past cylinders and spheres," *J. Non-Newtonian Fluid Mech.*, vol. 29, pp. 381-432, 1988.
- [32] A. Afonso, M. A. Alves, F. T. Pinho, and P. J. Oliveira, "Uniform flow of viscoelastic fluids past a confined falling cylinder," *Rheol. Acta*, vol. 47, pp. 325-348, 2008.
- [33] G. R. Moss and J. P. Rothstein, "Flow of viscoelastic wormlike micelle solutions through a periodic array of cylinders." *J. Non-Newtonian Fluid Mech.*, vol. 165, pp. 1-13, 2010.
- [34] A. A. Dey, Y. Modarres Sadeghi, and J. P. Rothstein, "Experimental observation of viscoelastic fluid structure interactions." *Journal of Fluid Mechanics*, vol. 813, 2017.